Journal of the Korean Nuclear Society
Volume 34, Number 4, pp.382~395, August, 2002

Transient Critical Heat Flux Under Flow Coastdown in a Vertical Annulus With Non-Uniform Heat Flux Distribution

Sang-Ki Moon, Se-Young Chun, Ki-Yong Choi, and Won-Pil Baek
Korea Atomic Energy Research Institute
150 Dukjin-dong, Yuseung-gu, Daejon, 305-353 Korea
skmoon@kaeri.re.kr

(Receved August 29, 2001)

Abstract

An experimental study on transient critical heat flux (CHF) under flow coastdown has been performed for the water flow in a non-uniformly heated vertical annulus under low flow and a wide range of pressure conditions. The objectives of this study are to systematically investigate the effect of the flow transient on the CHF and to compare the transient CHF with steady-state CHF. The transient CHF experiments have been performed for three kinds of flow transient modes based on the coastdown data of a nuclear power plant reactor coolant pump. At the same inlet subcooling, system pressure and heat flux, the effect of the initial mass flux on the critical mass flux can be negligible. However, the effect of the initial mass flux on the time-to-CHF becomes large as the heat flux decreases. The critical mass flux has the largest value for slow flow reduction rate. There is a pressure effect on the ratio of the transient CHF data to steady-state CHF data. Except under low system pressure conditions, the flow transient CHF was revealed to be conservative compared with the steady-state CHF data. Bowring CHF correlation and thermal hydraulic system code MARS show promising results for the prediction of CHF occurrence.

Key Words : critical heat flux (CHF), flow transient, flow coastdown, annulus, non-uniform axial heat flux distributions, area split method using MARS code

1. Introduction

Presently, many aspects of the CHF phenomena are well understood and several reliable prediction methods are available for most of the operating conditions of nuclear reactors. However, the CHF behaviors in low-flow and high-pressure conditions are not well identified, which are of importance in the safety of nuclear reactors during high-pressure core inventory boil-off and fuel rod dryout situations that may occur during a small break loss-of-coolant accident (SB LOCA) or an anticipated transient without scram (ATWS). Furthermore, the CHF under low flow conditions plays an important role in thermal hydraulic behavior for research reactors and advanced nuclear reactors as well as

in the accident analyses of LWR. However, most of the experimental studies for CHF under low flow conditions have been performed under an atmospheric pressure condition. Therefore, it is necessary to systematically investigate the pressure effect on the CHF under low flow conditions and expand the low flow CHF database for a wider range of system pressure conditions.

In a nuclear reactor core, the CHF is more likely to happen during abnormal transients or accident conditions rather than during normal or steady-state conditions. Therefore, the understanding of the effects of transients on the CHF is very important for studying the CHF of nuclear power plants [1]. During abnormal or accident conditions of a nuclear reactor core, there are three different types of transients: flow rate transients, pressure transients and power transients. These three types of transients generally take place at the same time during abnormal transients or accident conditions, and thus the transient CHF phenomena would become more complicated.

The research on the transient CHF until now has been focused on the effect of the magnitude of transients and prediction methods for transient CHF using correction factors to the steady-state correlation [2-6]. Iwamura [2] carried out rapid flow transient tests using tube and annular test sections under system pressures of 0.5 ~ 3.9 MPa and flow reduction rates of 0.6 ~ 35 %/s. His results showed that critical mass flux at the inlet was larger than that of a steady-state mass flux even in low system pressure conditions. Celata et al. [3] performed transient CHF experiments by simultaneous variations of either two of three parameters among pressure, flow rate and heat flux with Freon 12. Their experimental data revealed the general inadequacy of using the steady-state CHF correlations at inlet conditions in predicting transient conditions. Cumo et al. [4] carried out flow transient CHF experiments and presented a transient CHF correlation using a correction factor to the steady-state CHF. Chang et al. [5] proposed a transient CHF regime map and derived transient CHF correction factors for each CHF regime using the local microlayer depletion factor and the upstream effect factor. However, these previous studies on the transient CHF were focused on somewhat large initial mass flux conditions. Leung [6] and Chang et al. [7] published an excellent review and summary of transient CHF.

Recently, the present authors have performed a CHF experiment using a vertical annulus test section with non-uniform axial heat flux in low-flow and wide pressure conditions [8]. As an extension of the steady-state CHF experiments, this paper shows the results of the flow transient CHF experiment. Flow coastdown of the reactor coolant pump has been simulated to investigate the flow transient effects on CHF, to compare the flow transient CHF data with the steady-state CHF data and to investigate the applicability of steady-state CHF correlations for flow transient conditions. The initial mass fluxes chosen in the present experiments do not correspond with those in typical PWR normal operating conditions. Thus, we do not simulate the magnitude of mass flux in typical PWR normal operating conditions but the coastdown trends only under low initial mass flux conditions.

2. Test Description

Figure 1 shows a schematic diagram of the test facility where the present CHF experiments are performed. It consists of a main circulating pump, orifice flow meters, a preheater, a CHF test section, a steam/water separator, a condenser, a pressurizer and a cooler. The flow rate of the test section inlet is controlled by the adjustment of the motor speed of the main circulating pump, the flow control valve and the bypass control valve. A

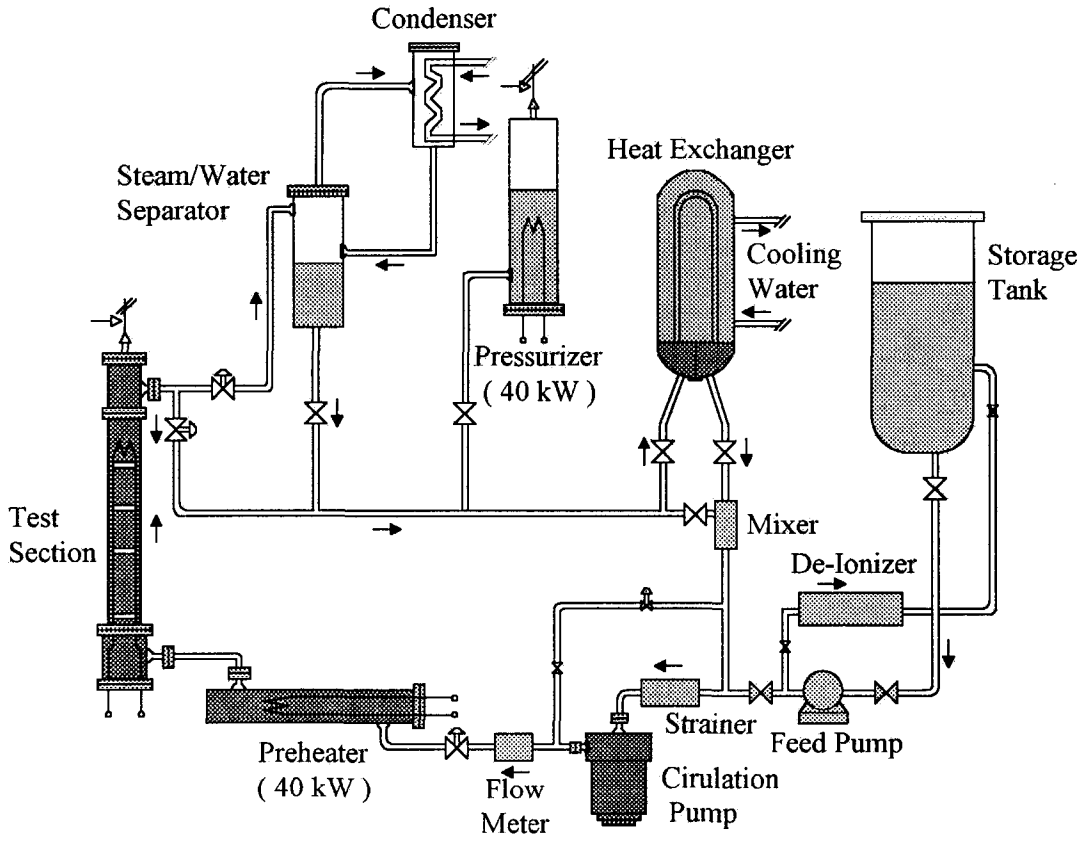

Fig. 1. KAERI RCS Loop Schematics

throttling valve located upstream of the test section inlet effectively suppresses the flow oscillations that are usually observed in low flow conditions. The preheater with power of 40 kW adjusts the degree of inlet subcooling of water entering the test section. The steam generated in the test section is condensed through the condenser attached in the steam/water separator. The system pressure defined as test section inlet pressure is maintained at a setting value using the pressurizer with an immersion heater with power of 40 kW. Three kinds of orifice flow meters with different measuring ranges are installed to measure the flow rate of water entering the test section.

As shown in Fig. 2, the annular test section consists of an outer pipe with a 19.4 mm inside diameter and an inner heater rod with a 9.53 mm outer diameter. The inner heater rod is heated indirectly by AC power using a silicon controlled rectifier (SCR) power control system. Six K-type thermocouples with a sheath diameter of 0.5 mm are embedded on the surface of the heater rod to measure the surface temperatures of the heater rod and to detect CHF occurrence. The inner rod having a heated length of 1843 mm is uniformly divided into ten steps to simulate a symmetric chopped cosine axial heat flux profile, as shown in Fig. 3.

In order to compare with steady-state CHF data, the inlet subcooling, inlet pressure and average heat flux for transient CHF test have the same

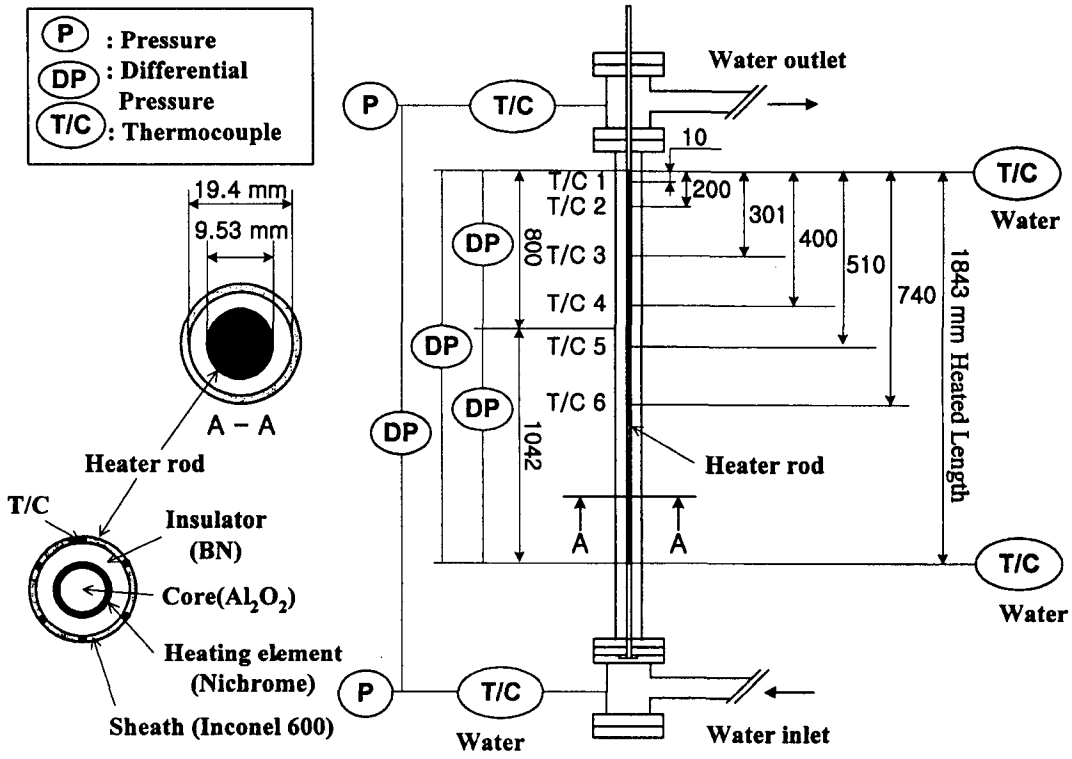

Fig. 2. Test Section Geometry and Thermocouple Location

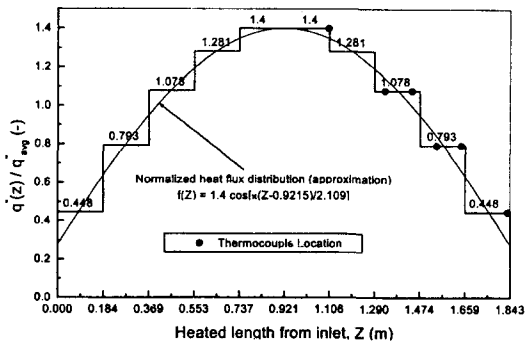

Fig. 3. Heat Flux Profile of Test Section

values with the steady-state CHF data [8]. However, the initial mass flux for flow transient CHF test has a larger value than for the steady-state CHF data. The CHF experiments are performed by the following procedures. After setting the initial mass flux, inlet subcooling, pressure and average heat flux at the desired values, only the flow rate is decreased by speed control of the main coolant pump according to the required transient mode. The flow coastdown continues until maximum wall temperature exceeds a predefined value. After that, the test section flow rate is increased to protect the test section from failure due to any excursive temperature rise. During each transient simulation, the system parameters such as system pressure, inlet water temperature and heat flux are maintained with constant values. In the present experiments, the CHF condition was determined when one of the surface temperatures of the heater rod increased sharply and then became

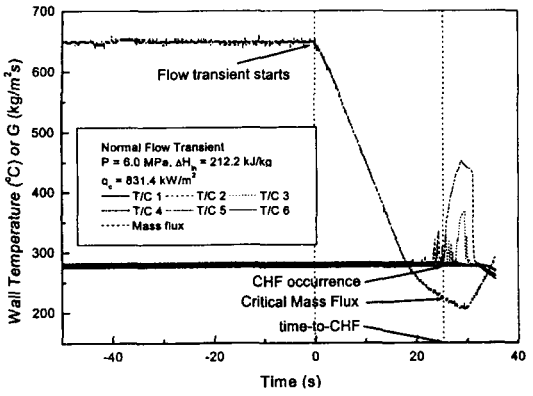

Fig. 4. Typical Variations of Heater Wall Temperature and Mass Flux During Tests

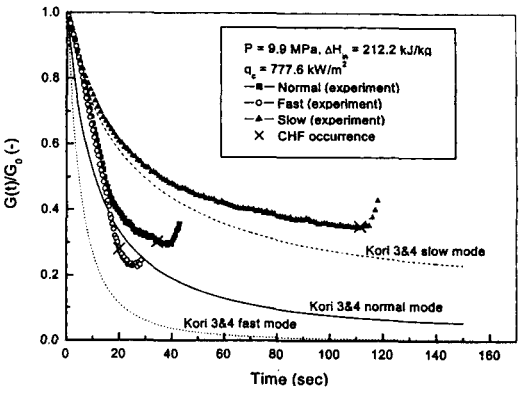

Fig. 5. Time-to-CHF Against Flow Transient Modes

110 K higher than the saturation water temperature. Figure 4 shows the typical variations of the heater wall temperature and mass flux during flow transient CHF tests. The time-to-CHF is defined as the time duration from the start of flow coastdown to the excursion of heater rod wall temperature. Critical mass flux is defined as the inlet mass flux at the CHF occurrence (i.e., at time-to-CHF).

Using the test section with a non-uniform axial heat flux, a total of 118 CHF data for three kinds of transient modes (i.e., slow, normal and fast flow coastdown) have been collected for inlet water subcooling ranging from 86 to 353 kJ/kg, initial mass fluxes of 650 and 550 kg/m^{2}s, system pressure (test section inlet pressure) from 0.54 to 10.48 MPa, exit quality from 0.02 to 0.63, and time-to-CHF of 2.38 to 177.78 seconds. About 72 % of CHFs occur at thermocouple No. 2 located 200 mm upstream from the exit of the test section. The uncertainties of the measuring system are estimated from the calibration of the sensors and the accuracy of equipment system, according to ANSI/ASME PTC 19.1 code [9]. The evaluated uncertainties in the measurements are less than ± 0.3 %, ± 1.5 %, ± 0.6 % and ± 1.8 % of the readings for pressure, flow rate, temperature and power, respectively. The measured data are recorded, processed and stored in a data acquisition and control unit.

Figure 5 shows actual flow coastdown trends compared with the reactor coolant pump of Kori 3 and 4 nuclear power plants. Here, a normal mode means a similar coastdown curve of Kori 3 and 4 nuclear power plants. The fast and slow modes simulate the square and the square root of the normal coastdown curve. As shown in Fig. 5, the fast and normal modes of the flow transient do not have the same coastdown curve as Kori 3 and 4 due to the limitation of the speed control of the main circulation pump, and interactive effects between the flow rate and the pressure drop in the present experimental loop.

3. Experimental Results

3.1. Parametric Trends

As shown in Fig. 4, as the inlet mass flux decreases, the heater wall temperature increases abruptly when the CHF condition is reached. When the flow regimes of the present CHF data are assessed as rough estimates by the conventional flow regime map for round tubes

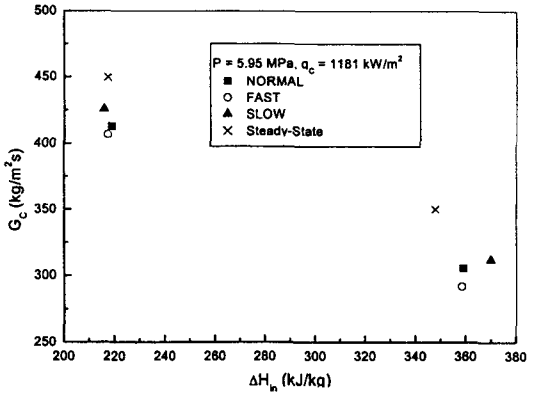

Fig. 6. Effect of Inlet Subcooling on Critical Mass Flux

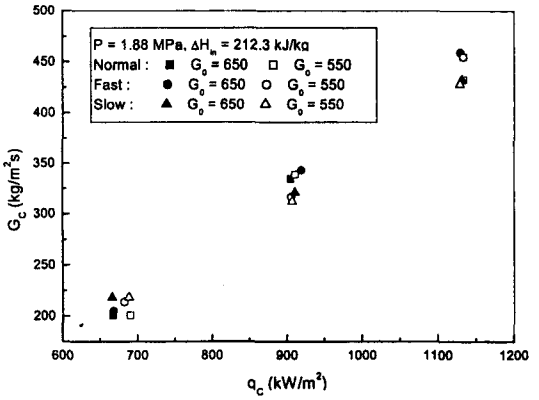

Fig. 8. Effects of Initial Mass Flux and Applied Heat Flux on Critical Mass Flux

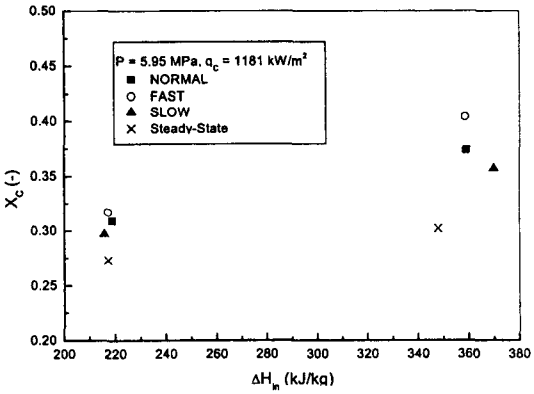

Fig. 7. Effect of Inlet Subcooling on Critical Exit Quality

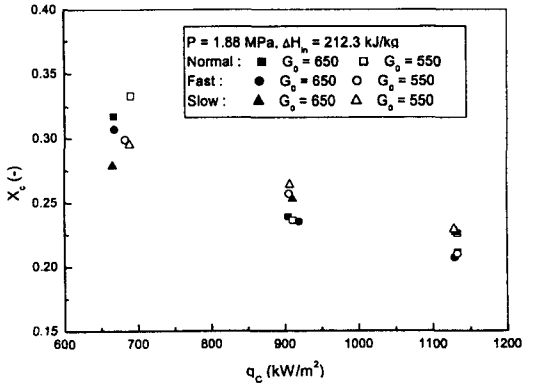

Fig. 9. Effects of Initial Mass Flux and Applied Heat Flux on Critical Exit Quality

[10], the flow regimes are revealed to be annular-mist flows. This means that the CHF occurs when the liquid film is dried out by depletion on the surface of the heater rod.

Figure 5 shows the time-to-CHF for three flow transient modes at the same inlet subcooling, test section average heat flux and system pressure. As shown in the figure, the fast flow transient has the smallest time-to-CHF whereas the slow flow transient has the largest time-to-CHF. However, the fast flow transient has the smallest critical mass flux (defined as the mass flux when the CHF occurs) whereas the slow flow transient has the largest critical mass flux. Usually, these critical mass fluxes are lower than those of the steady-state CHF conditions at the same system pressure, inlet subcooling and average heat flux.

Figures 6 and 7 show the critical mass flux and the critical exit quality as a function of inlet subcooling for three flow transient modes at the same system pressure and heat flux. As shown in the figures, the critical mass flux should be decreased in order to induce a CHF as inlet subcooling increases for a fixed average heat flux

and system pressure. Also, critical exit quality will increase due to the decrease of the critical mass flux, as can be seen by heat balance for the test section. The fast transient has the smallest critical mass flux and thus, the largest critical exit quality. On the other hand, the slow transient has the largest critical mass flux and the smallest critical exit quality.

Figures 8 and 9 show the effect of the initial mass flux on the flow transient CHF. As the test section average heat flux (i.e., test section power) increases, the critical mass flux increases and the critical exit quality decreases. Even if the initial mass fluxes of 550 and 650 kg/m^{2}s are somewhat different, there is no significant difference in the critical mass flux. For a fixed test section power and inlet subcooling, the initial exit quality at the lower mass flux of 550 kg/m^{2}s is 1.3 to 3 times larger than that for high mass flux of 650 kg/m^{2}s. However, the critical exit qualities show similar values for both conditions. The main effect of the initial mass flux is on the time-to-CHF as shown in Fig. 10. The time-to-CHF for the lower initial mass flux is about 76 % smaller than that for the higher initial mass flux, because the critical mass fluxes are almost the same but the initial mass flux are different. A higher average heat flux would result in a larger critical mass flux and smaller time-to-CHF, and the time to reach the same mass flux is not so different in the early phase of the flow transients. Thus, the effect of the average heat flux on the time-to-CHF becomes small as the test section average heat flux increases. Iwamura also observed similar results, in that the initial mass velocity ranging from 660 ~ 1600 kg/m^{2}s had little effect on flow reduction CHF characteristics [2].

3.2. Comparison with Steady-State CHF

The present flow transient CHF data have been compared to the steady-state CHF data that were obtained using the same test section [8]. Figure 11 shows the critical mass flux ratio against system pressure for three flow transient modes. Here, the subscripts FT and ST denote the flow transient and the steady state, respectively. As shown in the figure, at low system pressure, the critical mass flux for the flow transients has a higher value than that for the steady-state CHF condition. This might be a premature CHF due to some instability that usually occurs in low-pressure and low-flow conditions. However, at higher system pressures, the critical mass flux for the flow transient has a

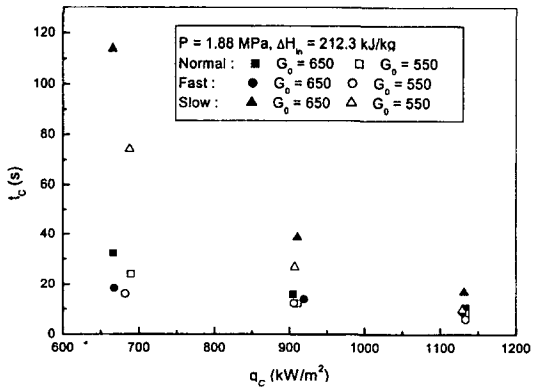

Fig. 10. Effect of Initial Mass Flux on Time-to-CHF

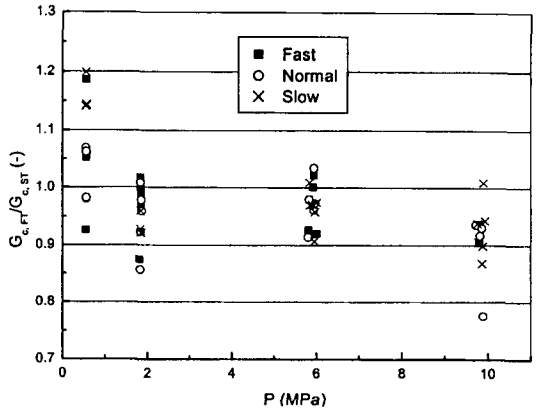

Fig. 11. Comparison of Critical Mass Flux for Flow Transient CHF with Steady-State CHF

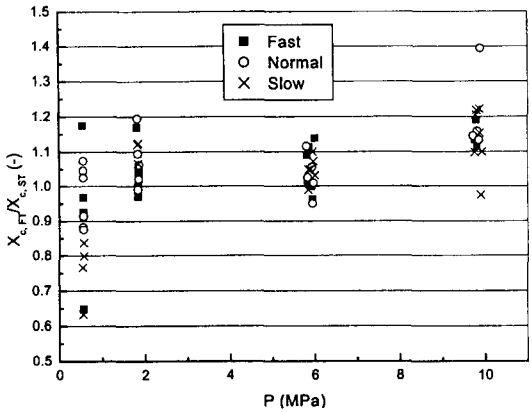

Fig. 12. Comparison of Critical Quality for Flow Transient CHF with Steady-State CHF

lower value than that for the steady-state CHF condition. Also, as shown in Fig. 12, except for low system pressure, most of the critical exit qualities for the flow transient have higher values than those for the steady-state CHF condition. Therefore, in the viewpoint of a thermal margin of nuclear reactor, the flow transient CHF is conservative except under the low system pressure conditions. Here, the conservatism means that the flow transient CHF is higher than in steady-state conditions under the same operating conditions of inlet subcooling, inlet mass flux and system pressure.

Iwamura [2] indicated that the critical mass flux ratio between flow transient and steady state depended mainly on the system pressure. The critical mass flux ratio was unity below a threshold flow reduction rate and decreased from unity over the threshold value. At the higher system pressure, the threshold flow reduction rate became greater and a variation of the critical mass flux ratio smaller. However, if we examine their data in detail, some data of the critical mass flux ratio are larger than unity at low system pressure and small flow reduction rate, although it is not so clear. Overall, the results showed that the flow transient CHF characteristics at low system pressure are very different from those of high system pressure. Including Iwamura's experimental study [2], most of the previous flow transient experiments have been performed at higher initial mass flux and larger flow reduction rate than the present experiment. Thus, the flow transient CHF characteristics in low initial mass flux and low system pressure need to be investigated more systematically.

4. Prediction of Flow Transient CHF

4.1. Prediction Results of Conventional CHF Correlation Using Inlet Mass Flux

In flow transient CHF experiments, it is difficult to obtain the local parameters because the local mass flux can be different from the inlet mass flux due to some time delay between inlet and any local point. Thus, in general, transient thermal-hydraulic codes are used to obtain local and instantaneous parameters at CHF locations. However, the accuracy of local two-phase flow parameters depends on the model and calculation scheme used in the codes and it is difficult to verify quantitatively the calculation results because direct measurements of transient two-phase flow parameters are extremely difficult [2].

However, such a time delay is remarkable only for very fast flow transient conditions. By preliminary analyses for the present CHF data, it was possible to assume that there is no significant time delay in local mass flux in the present experimental conditions. Therefore, we can calculate local parameters for a whole test section using inlet conditions such as fluid temperature and mass flux. Based on this assumption, we compared the present CHF data with Bowring CHF correlation [11] since it showed a reasonable prediction result for steady-state low-flow CHF

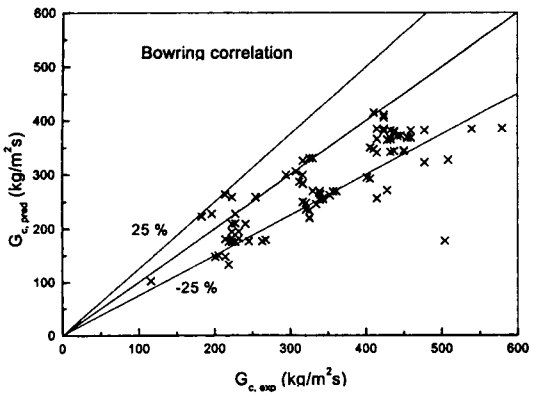

Fig. 13. Critical Mass Flux Prediction Results

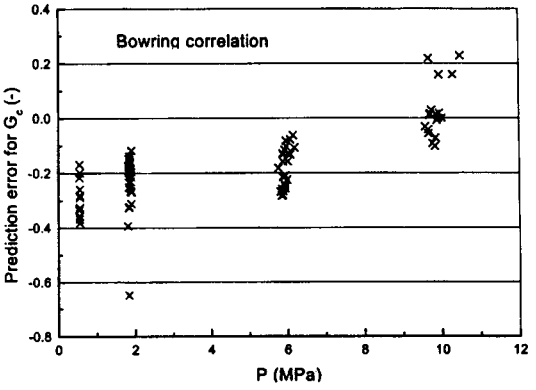

Fig. 15. Critical Mass Flux Prediction Results

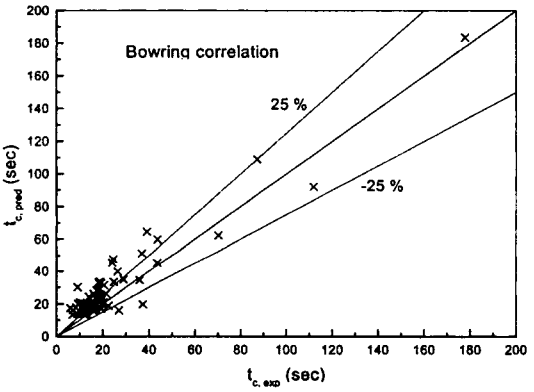

Fig. 14. Time-to-CHF Prediction Results

data [12]. However, still, this correlation overestimated the CHF under low system pressure conditions for steady-state low-flow CHF data. The flow transient CHF conditions are calculated as follows: Given the total power and the axial heat flux distribution, local parameters such as heat flux and quality at each time of flow transient are calculated at each location Z where the test section is uniformly divided into 100 locations from inlet to exit. In a preliminary study, the step size (18.43 mm) was found not to affect the CHF prediction results. Using the Bowring CHF correlation, a local CHF value is calculated at each time and each location Z using the local conditions calculated before. If the local heat flux is equal to the local CHF value that is predicted by the CHF correlation, it is judged that the CHF occurs at that location and at that time. Otherwise, the calculation proceeds to the next time step. If the CHF does not occur until the termination of the flow transient, the inlet mass flux is assumed to decrease following flow transient curves and the above calculation procedure continues until CHF occurrence.

Figures 13 through 15 show the prediction results for critical mass flux and time-to-CHF using Bowring correlation [11]. As shown in the figures, the critical mass flux is underestimated, and the time-to-CHF is overestimated. Thus, the flow transient CHF conditions are predicted to occur later than the experimental data. As shown in Fig. 15, Bowring correlation shows better prediction results as the system pressure increases. The worse prediction results at low system pressure might be due to the worse prediction capability of the correlation at low system pressure rather than the flow transient itself. The prediction results become better at high quality, high system pressure and slow transient mode. As the flow transients become faster, in general, the difference

between inlet and exit mass fluxes become large. Thus, for fast transients, there are larger delays in local mass flux and quality than in slow transient conditions. This might be the cause of the worse prediction results for fast transients.

4.2. Prediction Results Using Thermal Hydraulic System Code MARS

Annular flow in annulus geometry is characterized as two liquid films flowing along the inner heated rod and outer unheated wall. Critical heat flux occurs when the liquid film on the inner heated rod dries out, while there still exists the liquid film on the outer unheated wall. It was found that one-dimensional modelling of a thermal hydraulic system code, MARS [13], cannot distinguish such a film split phenomena in annular geometry, resulting in overestimation of the onset of CHF [14]. Recently, Chun et al. [15] presented a three-dimensional mechanistic modelling method to overcome the problem and obtained enhanced prediction capability. However, the film dryout model is a complex function of film flow rate and other parameters, and more improvement is necessary for better prediction accuracy. It is thought that one-dimensional modelling also can be used to estimate the onset of critical heat flux with good prediction capability if proper modification on modelling annulus geometry is taken. In this work, a different approach is taken to deal with the film split phenomena in annular geometry. This concept is based on the premise that liquid flow entering the test section is split into two regions and CHF occurs when the liquid film on the inner heating rod side is dried out.

The test section is non-uniformly nodalized to have 40 nodes in total. The upper half region of the test section in which CHF is predicted to occur, has more fine nodes than the lower half

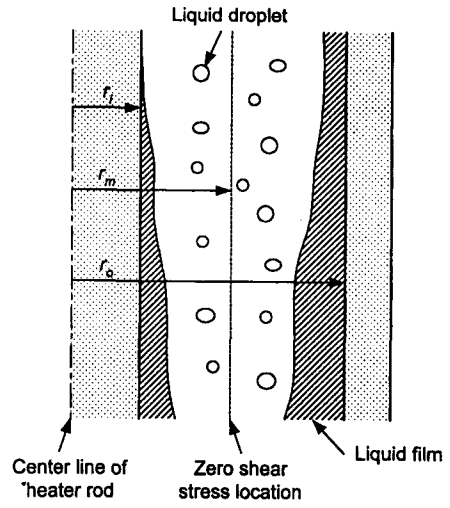

Fig. 16. Schematic Diagram of Annular Two-Phase Flow in Annulus

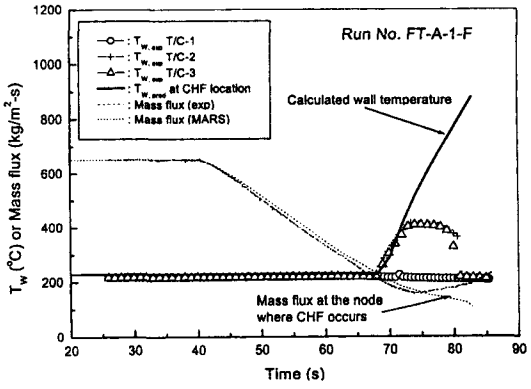

Fig. 17. Critical Mass Flux Prediction Result Using MARS Code

region [16]. An area split approach taken in this study focuses on the split of the liquid film on the inner heated rod rather than the film on the outer unheated wall. From the viewpoint of CHF, the inner liquid film plays a critical role, because the CHF occurs when the inner film is dried out. It is thus assumed that the annular flow area can be divided into two regions: an inner flow area where the inner liquid film flows, and an outer flow area

Table 1. CHF Prediction Results Using MARS Code

Run No.	P (MPa)	$G_{c,exp}$ (kg/m^{2}s)	$G_{c,pred}$ (kg/m^{2}s)	G_{error} (%)	$t_{c,exp}$ (s)	$t_{c,pred}$ (s)	$t_{c,error}$ (%)
FT-C-3-F	0.5	521.7	350.0	-32.9	9.0	22.8	153.3
FT-C-4-F	0.6	267.5	186.6	-30.3	25.0	34.2	36.8
FT-A-1-F	1.9	205.1	229.5	11.9	28.5	28.0	-1.8
FT-A-4-F	1.9	223.0	241.9	8.5	27.0	26.8	-0.7
FT-A-7-F	1.9	338.9	293.4	-13.4	21.0	25.2	20.0
FT-A-8-F	1.8	459.3	366.0	-20.3	13.5	24.0	77.8
FT-A-11-F1	1.8	419.2	328.2	-21.7	14.5	23.2	60.0
FT-B-2-F	5.9	245.2	304.5	24.2	27.0	23.0	-14.8
FT-B-7-F	5.8	325.5	330.2	1.4	21.0	21.0	0.0
FT-B-9-F	6.1	231.9	328.9	41.8	27.0	22.6	-16.3
FT-B-11-F	5.9	437.0	504.1	15.4	14.5	11.0	-24.1
FT-D-2-F	9.7	325.5	448.0	37.6	7.0	5.0	-28.6
FT-D-6-F	9.8	423.6	498.4	17.7	15.0	3.0	-80.0

Table 2. Prediction Error for Critical Mass Flux of MARS Code Default Calculation and the Present Area Split Method

Error (%)	MARS code default calculation	Present area split method
Mean Error	-55.8	3.1
Absoulte Error	55.8	21.3
RMS Error	59.3	25.1

where the outer liquid film flows. The boundary between the two areas is based on the radial location at which the interfacial shear stress becomes zero as shown in Fig. 16. A radial location where the interfacial shear stress becomes zero is given by Kirillov [17]:

$$r_m = \sqrt{\frac{r_o^2 - r_i^2}{2\log(r_o / r_i)}}, \qquad (1)$$

where r_i is the radius of the inner heater rod and r_o is the radius of the outer cold wall. Using the above equation, the inner flow area has 38.5 % of the total annular flow area. The inlet mass flux is also split into two areas based on $r = r_m$. It is assumed that the same ratio of area split rate can be applied to the inlet mass flux in the inner area. Therefore, 38.5 % of the inlet mass flux is used for code input in MARS.

Local parameters such as local quality, mass flux and wall temperature of the heater rod are predicted using the MARS code. Figure 17 shows the wall temperature trace and the excursion of wall temperature (i.e. CHF occurrence) coincides with the experimental data. Table 1 shows the

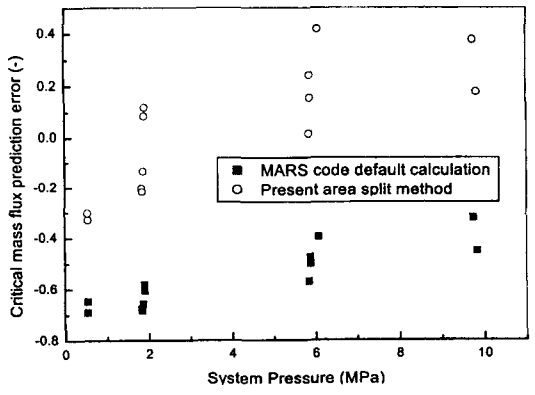

Fig. 18. Critical Mass Flux Prediction Error Against System Pressure

prediction results for critical mass flux and time-to-CHF. It is evident that there exists a pressure effect on the calculation results. For low system pressure of about 5 bar, the area split method underestimates the critical mass flux. On the other hand, it overestimates the critical mass flux for high system pressure of about 90 bar. However, the prediction errors do not seem to be great compared with the default code calculation, which always underestimates the critical mass flux. Table 2 and Fig. 18 show the prediction errors for the critical mass flux of the MARS code default calculation and the present area split method. Therefore, it can be concluded that CHFs occurring in annular geometry can be reasonably well predicted if the flow area and inlet mass flux are reduced according to the location of zero interfacial shear stress.

5. Conclusions

CHF experiments were conducted to observe the effects of flow transients on the CHF and to compare the flow transient CHF data with the steady-state CHF data in an annulus having a non-uniform heat flux profile under low flow and a wide range of pressure conditions. From the experiments, the following conclusions have been obtained:

- For the present experimental conditions, most of the critical mass fluxes at flow transients have smaller values than steady-state CHF data. Thus, even if at the same system pressure, inlet subcooling and heat flux, the CHF is delayed at flow transients. Therefore, flow transient CHF is conservative compared with steady-state CHF data except under low system pressure conditions.
- For low system pressure, the critical mass flux for flow transients has a somewhat larger value than the steady-state CHF condition. This might be a premature CHF due to an instability that usually occurs under low-pressure and low-flow conditions.
- The Bowring correlation shows better prediction results for high system pressure, high quality, and slow transient modes rather than for low system pressure, low quality and fast transient modes.
- The thermal hydraulic system code MARS shows a promising prediction result for the heater wall temperature trends. Therefore, it can be concluded that CHFs occurring in annular geometry can be reasonably predicted if the flow area and inlet mass flux are split according to the location of zero interfacial shear stress.

Acknowledgment

This work was performed under the Long-term Nuclear R&D Program sponsored by the Ministry of Science and Technology of Korea.

Nomenclature

G	Mass flux
P	System pressure
q_{avg}	Average heat flux for whole heated length
$q(Z)$	Local heat flux at Z
q_c	Critical heat flux (average heat flux at CHF from inlet to exit)
r_i	Radius of inner heater rod
r_m	Radius at zero interfacial shear stress
r_o	Radius of the inner surface of outer unheated wall
T_w	Heater wall temperature
t	Time
t_c	Time-to-CHF
X_c	Thermodynamic quality at exit (critical quality)
Z	Axial location from inlet

Greeks

ΔH_{in} Inlet subcooling

Subscripts

c CHF or critical
error Prediction error
exp Experiment
FT Flow transient
0 Initial
pred Predicted
ST Steady state

References

1. S. H. Chang and W. P. Baek, "Perspective on Critical Heat Flux Research for Nuclear Reactors," Proc. of NTAHAS 98: First Korea-Japan Symposium on Nuclear Thermal Hydraulic and Safety, Pusan, Korea, October 21-24 (1998).
2. T. Iwamura, "Transient Burnout Under Rapid Flow Reduction Condition," J. of Nucl. Sci. and Tech., 24[10], 811-820 (1987).
3. G. P. Celata, M. Cumo et al., "CHF Behavior During Pressure, Power and/or Flow Rate Simultaneous Variations," Int. J. Heat Mass Transfer, 34[3], 723-738 (1991).
4. M. Cumo, F. Fabrizi and G. Palazzi, "Transient Critical Heat Flux in Loss-of-Flow-Accidents (L.O.F.A)," Int. J. Multiphase Flow, 4, 497-509 (1978).
5. S. H. Chang, K. W. Lee and D. C. Groeneveld, "Transient-Effects Modeling of Critical Heat Flux," Nucl. Eng. Design, 113, 51-57 (1989).
6. J. C. M. Leung, "Critical Heat Flux Under Transient Conditions: A Literature Survey," ANL Report, ANL-78-39, NUREG/CR-0056 (1978).
7. S. H. Chang and W. P. Baek, "Critical Heat Flux - Fundamentals and Applications," Chungmoongak Pub. Co., Seoul (in Korean) (1997).
8. S. K. Moon, S. Y., Chun, H. J., Chung et al., "Effect of Axial Heat Flux Distributions on Critical Heat Flux under Low Flow and a Wide Range of System Pressures with Vertical Annulus," Proc. of 8th Int. Conf. on Nuclear Engineering, April 2-6, 2000, Baltimore, MD USA (2000).
9. ANSI/ASME PTC 19.1, "ASME Performance Test Codes, Supplement on Instruments and Apparatus, Part 1, Measurement Uncertainty" (1985).
10. K. Mishima and M. Ishii, "Flow Regime Transition Criteria for Upward Two-Phase Flow in Vertical Tubes," Int. J. Heat Mass Transfer, 27[5], 723-737 (1984).
11. R. W. Bowring, "A New Mixed Flow Cluster Dryout Correlation for Pressures in the Range 0.6-15.5 MN/m^2 (90-2500 psia) - for Use in a Transient Blowdown Code," Paper C217/77, Presented at Conf. On Heat and Fluid Flow in Water Reactor Safety, IMechE, Manchester, Sep. 13-15 (1977).
12. S. Y. Chun, H. J. Chung, S. K. Moon et al., "Effect of Pressure on Critical Heat Flux in Uniformly Heated Vertical Annulus under Low Flow Conditions," Nucl. Eng. Design, 203, 159-174 (2001).
13. W. J. Lee, B. D. Chung, J. J. Jeong and K. S. Ha, "Development of a Multi-Dimensional Realistic Thermal-Hydraulic System Analysis Code, MARS 1.3 and Its Verification," KAERI/TR-1108/98 (1998).
14. J. H. Chun, H. J. Chung, S. Y. Chun and U. C. Lee, "Assessment of MARS 1.4 Dryout Model Using KAERI Annular CHF Test," Proc. of the Korean Society of Mechanical Engineering Autumn Meeting (1999).
15. J. H. Chun, W. J. Lee, and U. C. Lee,

"Mechanistic Modelling of Annular Film Dryout in Annulus Geometry in MARS Code," Proc. of the Second Japan-Korea Symposium in Nuclear Thermal Hydraulics and Safety, Fukuoka, Japan (2000).

16. K. Y. Choi, S. K. Moon, S. Y. Chun and J. D. Jackson, "Prediction of Critical Heat Flux in a Non-Uniformly Heated Vertical Annulus Under Flow Transients Using an Area Split Approach," Proc. of '2001: A Nuclear Odyssey, ANS/HPS Conf., Texas, USA (2001).
17. P. L. Kirillov and I. P. Smogalev, "Calculation of Heat Transfer Crisis for Annular Two-Phase Flow of a Steam-Liquid Mixture Through an Annular Channel," AECL-4752 (1974).